# The Focal Form of Persistent Hyperinsulinemic Hypoglycemia of Infancy

## Morphological and Molecular Studies Show Structural and Functional Differences With Insulinoma

**Christine Sempoux,[1] Yves Guiot,[1] Karin Dahan,[2] Pierre Moulin,[1] Martine Stevens,[1] Virginie Lambot,[2] Pascale de Lonlay,[3] Jean-Christophe Fournet,[4] Claudine Junien,[5] Francis Jaubert,[6] Claire Nihoul-Fekete,[7] Jean-Marie Saudubray,[3] and Jacques Rahier[1]**

**Paternal mutation of ATP-sensitive $K^+$ ($K_{ATP}$) channel genes and loss of heterozygosity (LOH) of the 11p15 region including the maternal alleles of *ABCC8*, *IGF2*, and *CDKN1C* characterize the focal form of persistent hyperinsulinemic hypoglycemia of infancy (FoPHHI). We aimed to understand the actual nature of FoPHHI in comparison with insulinoma. In FoPHHI, the lesion consists in clusters of β-cells surrounded by non–β-cells. Compared with adjacent islets, proinsulin mRNA is similar and proinsulin production higher ($P \leq 0.02$), indicating regulation at a translational level, with slightly lower insulin stock and lower ABCC8 peptide labeling ($P<0.05$). Insulinomas, composed of β-cell nests or cords, have similar proinsulin mRNA compared with adjacent islets, highly variable proinsulin production, lower insulin stock ($P \leq 0.02$), and higher ABCC8 peptide labeling ($P<0.05$). Proinsulin mRNA is lower than in FoPHHI ($P<0.001$). Islets adjacent to FoPHHI appear to be resting, in contrast to those adjacent to insulinomas, evidencing intrapancreatic regulation of islet β-cell activity. IGF2 peptide is present inside and outside both lesions, but IGF2 mRNA is restricted to the lesions. The 11p15 LOH and absence of CDKN1C peptide staining are demonstrated in all FoPHHI but also in three of eight insulinomas. Despite some molecular similarities, FoPHHI is thus fundamentally different from insulinoma. *Diabetes* 52:784–794, 2003**

From the [1]Cliniques Universitaires St-Luc, Pathology, Brussels, Belgium; the [2]Cliniques Universitaires St-Luc, Genetics, Brussels, Belgium; the [3]Hôpital Necker-Enfants Malades, Pediatrics, Paris, France; the [4]Hôpital St-Justine, Pathology, Montréal, Quebec, Canada; the [5]Hôpital Necker-Enfants Malades, INSERM U383, Paris, France; the [6]Hôpital Necker-Enfants Malades, Pathology, Paris, France; and the [7]Hôpital Necker-Enfants Malades, Surgery, Paris, France.

Address correspondence and reprint requests to Christine Sempoux, MD, Department of Pathology (ANPS 1712), University Hospital, U.C.L. Avenue Hippocrate 10, B-1200 Brussels, Belgium. E-mail: christine.sempoux@anps.ucl.ac.be.

Received for publication 21 March 2002 and accepted in revised form 2 November 2002.

DIG, digoxigenin-11–2′deoxy-uridine-5′-triphosphate; FoPHHI, Focal persistent hyperinsulinemic hypoglycemia of infancy; $K_{ATP}$ channel, ATP-sensitive $K^+$ channel; LOH, loss of heterozygosity; PHHI, persistent hyperinsulinemic hypoglycemia of infancy; SB-P, streptavidin-biotin-peroxidase; SOD, specific optical density.

Two different histological forms of persistent hyperinsulinemic hypoglycemia of infancy (PHHI) have been recognized (1–4) with distinct therapeutic implications (5). The first one, diffuse PHHI, is mostly related to mutations in the genes coding for the sulfonylurea receptor (*ABCC8*, formerly *SUR1*; MIM: 600509) or the inward rectifying $K^+$ channel (*KCNJ11*, formerly *Kir6.2*; MIM: 600937) (6,7), the two β-cell membrane ATP-sensitive $K^+$ ($K_{ATP}$) channel subunits (8). The consequence of these mutations is a nonfunctional $K_{ATP}$ channel leading to continuous β-cell depolarization and inappropriate insulin secretion (9,10). The second form of PHHI, focal PHHI (FoPHHI), is cured by resecting a limited endocrine pancreatic lesion (5,11) composed of hyperplastic islets (1–4). FoPHHI is associated with a paternally inherited *ABCC8* mutation (less frequently, *KCNJ11*) (12,13) and with a specific loss, restricted to the lesion, of maternal alleles of the 11p15 region (14). This region includes the *ABCC8* and *KCNJ11* genes and also imprinted genes *H19*, *IGF2*, and *CDKN1C* (formerly $p57^{KIP2}$) implicated in cell proliferation regulation (15–17). FoPHHI is therefore not only characterized by a complete loss of $K_{ATP}$ channel function, resulting in insulin hypersecretion, but also by the development of a tumor due to imbalance between the imprinted genes mapped to 11p15. In agreement with this molecular concept, it has already been shown that the FoPHHI lesion has a higher β-cell proliferation index than islets from age-related control subjects (18,19). FoPHHI is found in 30–40% of PHHI patients (4,5); the incidence of PHHI in the general population varies between 1 in 30,000 and 1 in 50,000 (20).

Insulinomas can also cause severe hyperinsulinemic hypoglycemia. In contrast with FoPHHI, 11p15 loss of heterozygosity (LOH) has rarely been described in insulinomas (21,22), and their β-cell proliferation rate is usually low (18). The incidence of insulinomas in children and adolescents is very low, ~0.9 and 4.9%, respectively (23).

Our aim is to compare these two focal pancreatic endocrine lesions, FoPHHI and insulinoma, in their morphological characteristics, their reasons for insulin hypersecretion with the repercussions on their adjacent pancreas, and their mechanisms of tumoral development

TABLE 1
Clinical data of patients analyzed in this series

| | Age of onset | Age at surgery | Sensitivity to diazoxide | *ABCC8* paternal mutations |
|---|---|---|---|---|
| Focal PHHI (13) | | | | |
| 1 | 25 h | 1.5 months | − | 3165+1g>a |
| 2 | First hours | 2 months 2/3 | − | R842G |
| 3 | 1 h | 2 months 1/3 | − | R1494W |
| 4 | 1.5 months | 4 months | − | R1421C |
| 5 | 5 days | 6 months 1/2 | − | Not tested |
| 6 | First hours | 7 months | − | Not tested |
| 7 | 1 h | 5 months | − | Not tested |
| 8 | 3 h | 3.5 months | − | Not tested |
| 9 | First hours | 3 months | − | Not tested |
| 10 | First hours | 1.5 months | ? | 4138delCGAC-4138insGTG |
| 11 | 3 months | 4.5 months | − | Not tested |
| 12 | 2 days | 2 months | − | Not tested |
| 13 | 6 h | 3.5 months | − | G1555S |
| Insulinomas (8) | | | | |
| 14 | 5 years | 6 years | + | None found |
| 15 | 11 years | 12 years | + | Not tested |
| 16 | ? | 15 years | ? | Not tested |
| 17 | 29 years | 31 years | ? | Not tested |
| 18 | 29 years | 32 years | ? | Not tested |
| 19 | 43 years | 44 years | + | Not tested |
| 20 | 79 years | 79 years | ? | Not tested |
| 21 | 80 years | 81 years | + | Not tested |

Cases n°1–13 are FoPHHI and cases n°14–21 are insulinomas. Cases n°1, 2, 3, and 13 and the *ABCC8* mutations have previously been published by Fournet et al. (13).

in order to understand the nature of each one and to see whether it may be relevant to consider FoPHHI as an insulinoma of the infant.

## RESEARCH DESIGN AND METHODS

A total of 13 cases of FoPHHI in infants (1.5–7 months of age) suffering from severe diazoxide-resistant hypoglycemia of neonatal onset cured by partial pancreatectomy were compared with 8 insulinomas occurring in 3 children (6–15 years of age) and 5 adults (31–81 years of age) with recent onset hypoglycemia, 4 diazoxide-sensitive and 4 not tested (Table 1). All insulinomas were considered sporadic because of the complete absence of familial history of MEN1-associated tumors.

Samples containing both the lesion and its adjacent healthy islets were fixed in Bouin's solution for conventional microscopy and investigation of cellular endocrine composition, in 4% formalin to study ABCC8 and CDKN1C peptide expression as well as IGF2 peptide and mRNA expressions, and frozen in liquid nitrogen to search for 11p15 LOH. Analyses were performed on all cases containing sufficient material both inside and outside the lesion.

**Immunohistochemistry and in situ hybridization.** Immunohistodetections were performed to analyze endocrine cell composition of both lesions and adjacent islets as well as the presence of CDKN1C, ABCC8, and IGF2 peptides. Technical details are given in Table 2. Dr. M. Mikhailov and Prof. S.J. Ashcroft (Nuffield Department of Clinical Laboratory Sciences, John Radcliffe Hospital, Headington, Oxford, U.K.) provided the ABCC8 antibody. As the immunizing peptide was not available, its specificity was confirmed by documenting the absence of cross-reaction with SUR2 (cardiac muscle), CFTR, or MDR (exocrine pancreas and renal tumor, respectively).

To produce IGF2 probe, total RNA was extracted from snap-frozen pheochromocytomas (24) with Trizol reagent and reverse transcribed (Life Biotechnologies, Gibco-BRL, Merelbeke, Belgium). The specificity of primers used for human IGF2 amplification (positions 372-390 and 726-707 of the cDNA, accession no. XM_006402, NCBI nucleotide sequence) was checked by BLAST search on Genbank database. Sensitive IGF2 probe was produced by incorporation of digoxigenin-11–2′deoxy-uridine-5′-triphosphate (DIG) (Roche Diagnostics, Mannheim, Germany) during the PCR. Amplified DNA samples were quantified by a Gel Doc 2000 scanning device (Bio Rad, Nazareth, Belgium). IGF2 PCR product identity was confirmed by DNA

TABLE 2
Immunohistochemical stainings

| Analyses | Primary antibody/dilution | Detection system | Second primary antibody/dilution | Detection system |
|---|---|---|---|---|
| Hormonal composition | Anti-insulin(1) 1/2,000<br>Anti-glucagon(1) 1/900<br>Anti-somatostatin(1) 1/2,000 | SB-P-DAB | | |
| Densitometry | Anti-insulin 1/12,000 | SB-P-DAB | | |
| 11p15 LOH | Anti-*CDKN1C*(2) 1/100 | EnVision(3)-DAB | | |
| Volume densities | Anti-insulin 1/2,000 | SB-P-DAB | Anti-somatostatin 1/4,000 | APAAP-fast red |
| Golgi proinsulin/β cell area | Anti-proinsulin(1) 1/500 | SB-P-DAB | Anti-insulin 1/10 | SB-FITC |
| *ABCC8*/endocrine area | Anti-*ABCC8*(4) 1/250 | EnVision(3)-DAB | Anti-synaptophysin(3) 1/150 | SB-FITC |
| *IGF2*/endocrine area | Anti-*IGF2*(5) 1/200 | EnVision(3)-DAB | Anti-synaptophysin 1/150 | SB-FITC |

(1) Novo Biolabs, Bagsvaerd, Denmark; (2) NeoMarkers, Fremont, CA; microwave antigen retrieval; (3) Dako, Carpinteria, CA; (4) Provided by Dr. M. Mikhailov and Prof. S. J. Ashcroft, Nuffield Dept. of Clinical Laboratory Sciences, John Radcliffe Hospital, Headington, Oxford, U.K.; (5) Upstate Biotechnology, New York, NY; microwave antigen retrieval. SB; streptavidin-biotin; P: peroxidase; DAB: diaminobenzidine, dark chromogen; APAAP: alkaline phosphatase anti-alkaline phosphatase; Fast Red: Red chromogen; FITC: fluorescein isothiocyanate.

sequence analysis using a dye terminator sequencing system on the Genetic analyzer 3600 (Applied Biosystems, Foster City, CA).

Proinsulin mRNA was detected with a fluorescein isothiocyanate–labeled probe (final dilution 1:2; NCL-Proins, Novocastra, U.K.) (25). The DIG-labeled IGF2 probe (2.4 μg/ml, 18 h at 45°C) was detected with monoclonal anti-DIG antibody (1/50, 1 h, 30 min; Roche), and streptavidin-biotin-peroxidase (SB-P), followed by biotinylated tyramine amplification (1/800 during 9 min) (26), incubation with SB-P (1/800, 30 min), and diaminobenzidine (DAB) revelation system. In situ hybridization with unrelated probe against prostatic specific membrane antigen, also produced by DIG incorporation in PCR product, was included as negative control.

**Measurements.** β- and δ-cell volume densities (Vv) were measured by point-counting (27) on sections double-immunostained for insulin and somatostatin and expressed as the ratio of β-cell Vv–to–(β + δ) cell Vv.

An image analyzer measured β-cell crowding (number of β-cell nuclei/1,000 $\mu m^2$ of β-cell cytoplasm) (4). This parameter reflects the nucleo-cytoplasmic ratio: a low value indicating abundant cytoplasm, as observed in hyperfunctioning cells, and a high value characterizing packed resting cells. For these parameters, pancreases of 15 organ donors, deceased from causes unknown to affect endocrine pancreas, were used as age-matched controls (aged 2–9 months for infants and 9–72 years for insulinomas).

Intracellular insulin and proinsulin mRNA contents were quantified by densitometry (28) with an image analyzer IBAS 2000 (Zeiss-Kontron, Munich, Germany) and expressed as specific optical density (SOD).

Golgi proinsulin/β-cell area was evaluated on slides double-stained for proinsulin (immunoperoxidase) and insulin (immunofluorescence) digitized through a JVC KY-F58 color digital camera (Japan Victor, Brussels, Belgium). An image analyzer (KS-400 system; Zeiss-Vision, Munich, Germany) measured the surface ratio within both lesion and adjacent islets. ABCC8 and IGF2 peptide SODs were evaluated with the same devices with reference to the endocrine area labeled by immunofluorescence to synaptophysin.

**Statistics.** Results are given as median and range. The statistical significance of results between lesions and controls or with their adjacent islets are assessed by the Wilcoxon's rank-sum test and Wilcoxon's matched-pairs test, respectively.

**Microsatellite analysis.** LOH of the 11p15 region was searched in all but four (Table 1, n°1, 2, 3, 13) previously published cases of FoPHHI (13,14) and in all insulinomas. To evaluate the deletion size, 12 different microsatellite markers covering 20 Mb from 11p15.5 region (containing imprinted genes *H19*, *IGF2*, and *CDKN1C*) to 11p15.1 region (containing *ABCC8* and *KCNJ11*) were studied by PCR on either frozen material or microdissected slides of formalin-fixed specimens. Selected markers for the 11p15 region were from telomere to centromere (NCBI database): D11S922 (0.1 Mb), D11S4046 (0.8 Mb), tho (1.6 Mb), D11S1318 (2.1 Mb), D11S2351 (3.9 Mb), D11S1760 (4.2 Mb), D11S2071 (7.6 Mb), D11S569 (11.9 Mb), D11S1397 (15.0 Mb), D11S921 (16.1 Mb), D11S902 (16.3 Mb; intragenic in *ABCC8*), and D11S4114 (19.5 Mb). DNA was extracted from lesions and adjacent pancreas according to standard techniques. Fluorescent markers, custom synthesized by Genset (GensetOligos; Genset, Paris, France), were amplified using Amplitaq polymerase (Applied Biosystems). Gel data from PCR products were extracted and analyzed by an ABI 373 automated DNA sequencer and ABI Genescan software (Applied Biosystems).

## RESULTS

**Morphological description and cell composition.** In FoPHHI, the 13 lesions were usually invisible to the naked eye, measuring <10 mm. Microscopically ill delimited, the lesion seemed to result from the confluence of apparently normally structured islets separated by few exocrine acini maintaining a normal lobular pancreatic architecture (Fig. 1*A*). Endocrine cells, sometimes located in close contact with pancreatic ducts, were arranged in clusters of variable sizes separated by thin fibro-vascular strands or small cords of acinar tissue. Nuclei appeared polymorphous with size variations and hyperchromatism. Outside the lesion, islets were small with packed endocrine cells having scanty cytoplasm, thus showing a resting appearance (Fig. 1*C*). Immunohistochemistry revealed the presence of β-, α-, and δ-cells within the lesion, with non–β-cells predominantly localized at the periphery of the endocrine clusters, as in normal islets. Immunolabeling for insulin was homogeneous (Fig. 1*E*). Outside the lesion, labeling was more polarized and sometimes stronger. δ-Cells were particularly numerous in small islets (Fig. 1*G*).

Macroscopically, all insulinomas were well delimited, often palpable, recognizable and identifiable by their red-pink color. Their size varied from 8 to 24 mm. Microscopically the tumor was less well demarcated from adjacent pancreatic tissue, sometimes extending between exocrine acini or including normal islets. Endocrine cells were organized in nests (five cases) or ribbons (n°19, 20, 21: oldest patients), separated by fibrous and highly vascularized stroma (Fig. 1*B*). Three cases exhibited amyloid deposits in variable amounts (n°14, 15, 19). β-Cells were relatively uniform, cuboidal or cylindrical with moderately abundant acidophilic cytoplasm and a regular round or oval nucleus centrally located. The chromatin was granular, and there was a small nucleolus. Cellular and nuclear polymorphism was weak; mitoses and evidence of vascular invasion were absent. Outside insulinomas, islets showed regular nuclei and normally abundant cytoplasm and were thus very different from those located outside FoPHHI lesions (compare Figs. 1*C* and *D*). In the lesion, immunohistochemistry revealed almost exclusively β-cells, with either a diffuse and weak labeling for insulin or cellular variation in staining intensity (Fig. 1*F*). In three cases only (n°14, 16, 18), rare α- or δ-cells were scattered among tumoral β-cells. Islets outside insulinomas had much more intense insulin labeling and seemed relatively poor in δ-cells (Fig. 1*H*).

The differences in cell composition were quantified by measuring the volume density of β- and δ-cells. β-Cell Vv–to–(β + δ) cells Vv ratio was lower in FoPHHI than in insulinoma (0.93 [0.82–0.99] vs. 1.00 [0.99–1.00]; $P < 0.001$), implying that more δ-cells are present in FoPHHI. This ratio tended to be lower in islets located outside FoPHHI than in controls (0.55 [0.27–0.83] vs. 0.63 [0.44–0.77]). It was similar in islets adjacent to insulinoma and in their controls (0.87 [0.70–0.97] vs. 0.80 [0.70–0.92]).

**Insulin storage and proinsulin production.** In FoPHHI, insulin immunolabeling was similar or slightly weaker within the lesion than in adjacent islets (Figs. 1*E* and *G*). SOD measurements were not statistically different: 0.191 (0.123–0.171) in the lesion vs. 0.241 (0.121–0.268) in adjacent islets (Fig. 2*A*). In all insulinomas, insulin labeling was lower within the lesion than in adjacent islets (Figs. 1*F* and *H*). The difference estimated by measurement of insulin SOD was consistent (seven of seven cases) and large (0.114 [0.09–0.158] vs. 0.301 [0.185–0.345]; $P \leq 0.02$) (Fig. 2*A*).

In FoPHHI, proinsulin labeling was strong in all lesions and formed a dense crescent outlining the enlarged Golgi area, sometimes with a faint cytoplasmic labeling (Fig. 3*A*). In insulinomas, the staining was lower, restricted to a slightly enlarged Golgi area (Fig. 3*B*) except in three cases with a trabecular pattern, two exhibiting some cells with diffuse cytoplasmic labeling, and the third presenting diffuse cytoplasmic labeling of all tumoral cells. Outside both lesions, proinsulin labeling was rather weak and limited to a small Golgi area. In FoPHHI, measurements confirmed a larger Golgi proinsulin/β-cell area within the lesion ($n = 7$) than in β-cells of adjacent islets (0.420 [0.329–0.500] vs. 0.178 [0.109–0.356]; $P \leq 0.02$). No statis-

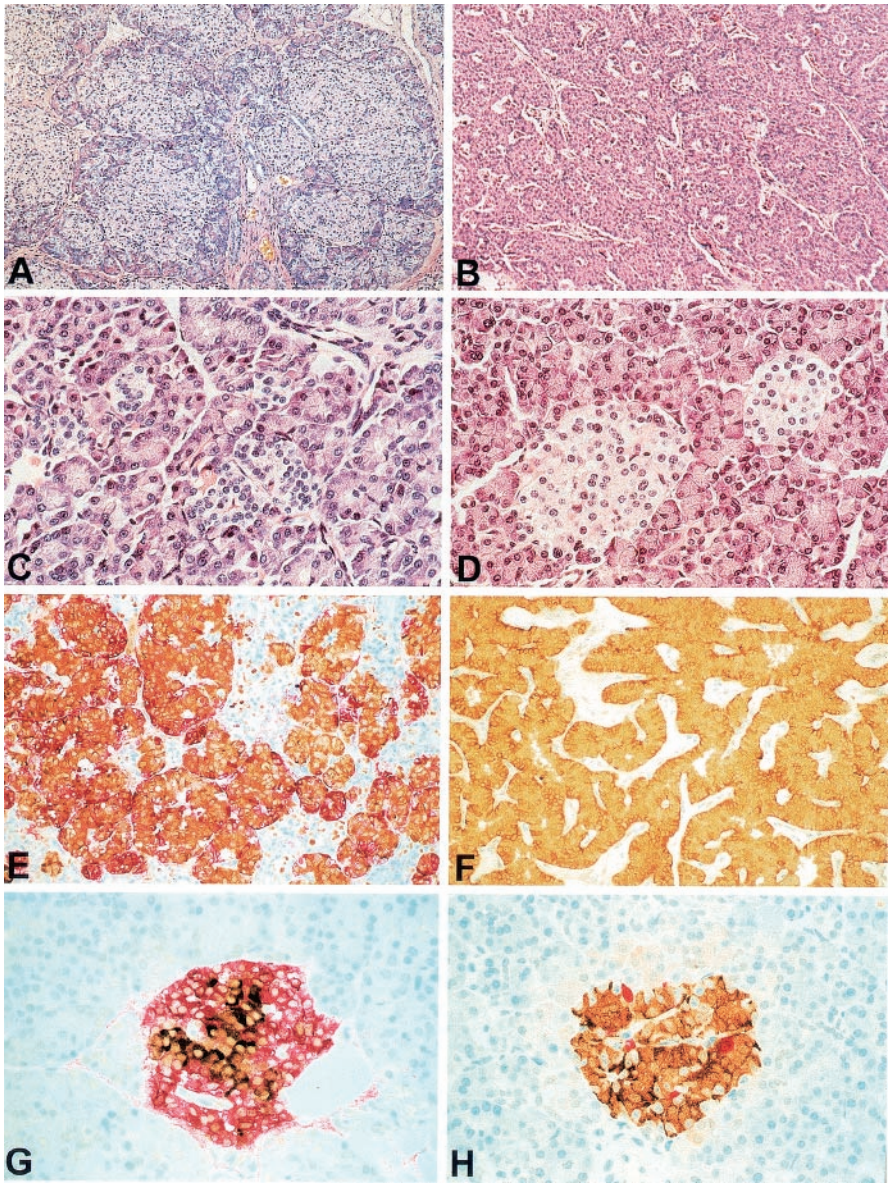


**FIG. 1. Morphological description and cell composition of the FoPHHI lesion (*A*, *C*, *E*, and *G*) and of insulinoma (*B*, *D*, *F*, and *H*). By conventional microscopy, the lesion responsible for FoPHHI (case n°5) consists in endocrine clusters of variable size, still delimited by a rim of exocrine tissue with preservation of intact pancreatic architecture (*A*: Hematoxylin-eosin ×63). Outside the lesion, islets are small with a resting appearance (*C*: Hematoxylin-eosin ×250). Double immunohistochemistry for insulin and somatostatin (case n°6), demonstrates spatial distribution of β-cells (in brown) disposed centrally and δ-cells (in red) peripherally in the clusters (*E*: immunoperoxidase and alkaline immunophosphatase ×125) as in normal islets. Outside the lesion, δ-cells sometimes seem particularly numerous in small islets (*G*: immunoperoxidase and alkaline immunophosphatase ×250). The intensity of insulin labeling is occasionally higher outside the lesion than inside (*E* and *G*). Conventional microscopy in insulinomas (case n°18) shows disappearance of normal pancreatic tissue. Tumoral endocrine cells are organized in nests scattered throughout a fibro-vascular stroma (*B*: Hematoxylin-eosin ×100). Outside the lesion, islets have a normal appearance (*D*: Hematoxylin-eosin ×250). Double immunohistochemistry for insulin and somatostatin (case n°21) shows that insulinomas are almost exclusively composed of β-cells, with a weak and variable insulin staining (*F*: immunoperoxidase and alkaline immunophosphatase ×125). Outside the lesion, insulin staining is much more intense within islets (*H*: immunoperoxidase and alkaline immunophosphatase ×250).**

tically significant difference between the lesion (0.254 [0.145–0.507]) and adjacent islets (0.132 [0.032–0.545]) was observed in insulinoma (Fig. 2*B*).

Proinsulin mRNA was detected in both types of lesions (Figs. 3*C* and *D*) and their adjacent islets. SOD was significantly higher in FoPHHI ($n = 7$; 0.348 [0.261–0.405]) than in insulinoma ($n = 4$; 0.135 [0.087–0.212]; $P < 0.001$). In contrast, there was no consistent difference between each lesion and their adjacent islets (FoPHHI: 0.336 [0.292–0.380] insulinoma: 0.216 [0.071–0.358]) (Fig. 2*C*).

The β-cell crowding reflects the cell activity, a low value indicating hyperfunctioning cells and a high value indicating resting cells. In FoPHHI ($n = 8$), crowding was significantly lower within the lesion (12.0 [10.3–13.9]) than in adjacent islets (15.2 [14.1–18.3]; $P < 0.02$), which had higher values than islets from age-matched controls (13.17 [11.23–15.58]; $P \leq 0.025$) (Fig. 2*D*). In insulinoma ($n = 7$), no significant difference was observed between the tumor (12.7 [11.0–13.9]), adjacent islets (11.5 [10.7–15.5]), and islets from age-matched controls (11.4 [9.8–12.1]) (Fig. 2*D*).

**ABCC8, IGF2, and CDKN1C peptide expression.** ABCC8 peptide was expressed as homogeneous cytoplasmic staining of endocrine cells in both types of lesions (Figs. 3*E* and *F*) and also in the adjacent pancreatic islets (Figs. 3*G* and *H*). In FoPHHI ($n = 7$), ABCC8 peptide staining was weaker than in adjacent islets in all but one lesion (n°2, missense paternal mutation of ABCC8), and SOD was indeed significantly lower in the lesion (0.018 [0.003–0.03]} vs. 0.029 [0.021–0.039]; $P < 0.05$) (Fig. 2*E*). In insulinomas, ABCC8 peptide SOD was significantly higher than in adjacent islets ($n = 7$; 0.043 [0.024–0.080] vs. 0.032 [0.011–0.047]; $P < 0.05$) (Fig. 2*E*).

IGF2 peptide was immunodetected in endocrine cells from FoPHHI and insulinomas with variable staining (Figs. 4*A* and *B*). IGF2 mRNA was detected in β-cells in both types of lesions (Figs. 4*C* and *D*). IGF2 peptide was also observed in islets outside both lesions where, importantly, IGF2 mRNA was undetectable. IGF2 peptide SOD was similar inside and outside lesions (FoPHHI, $n = 4$; 0.114 [0.083–0.126] vs. 0.121 [0.107–0.177]; insulinoma, $n = 4$; 0.110 [0.094–0.299] vs. 0.095 [0.079–0.104]).

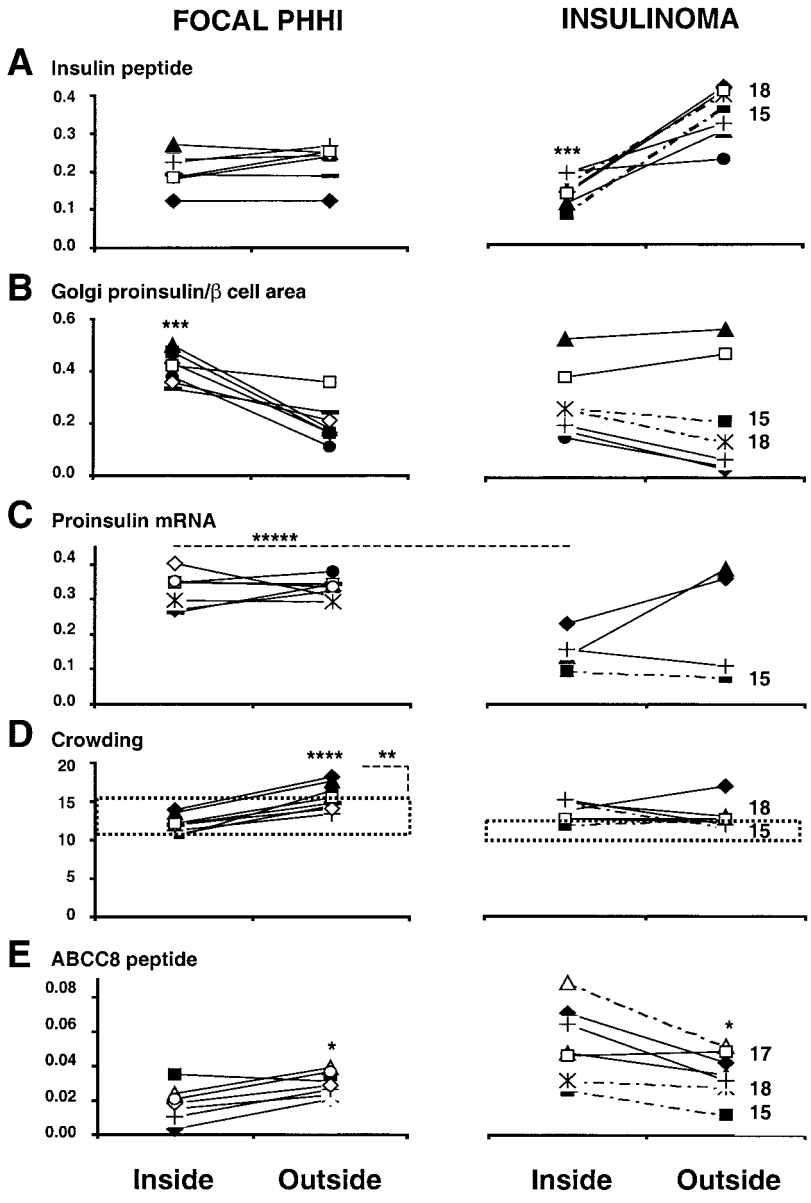


**FIG. 2. Morphological evaluation of functional characteristics inside and outside FoPHHI and insulinoma (case number and a dotted line show insulinomas with 11p15 LOH). *A*: Insulin storage. In FoPHHI, insulin peptide SOD is not statistically different within the lesion or in adjacent islets whereas in insulinomas it is significantly lower (***$P \leq 0.02$). *B*: Golgi proinsulin/β-cell area. Proinsulin labeling area is significantly increased in FoPHHI when compared with islets located outside the lesion (***$P \leq 0.02$), whereas in insulinomas the differences are not significant. *C*: Proinsulin mRNA production. Proinsulin mRNA SOD is higher in FoPHHI than in insulinoma (*****$P < 0.001$). There are no differences between each lesion and their respective adjacent islets. *D*: β-cell crowding (number of β-cell nuclei/1,000 μm$^2$ of cytoplasm). The crowding is significantly higher in islets located outside FoPHHI than in FoPHHI (****$P < 0.02$) and age-matched controls (dotted rectangle, **$P \leq 0.025$). In insulinoma, there is no significant difference between the tumor, islets outside the lesion, or islets from age-matched normoglycemic controls (dotted rectangle). *E*: ABCC8 peptide. ABCC8 SOD is significantly lower in FoPHHI than in adjacent islets (*$P < 0.05$), whereas it is significantly higher in insulinomas (*$P < 0.05$). For all of these parameters, no difference is observed between insulinomas with or without 11p15 LOH.**

CDKN1C peptide was completely absent from all tested cases of FoPHHI ($n = 9$) (Fig. 4*E*) but also from insulinomas with 11p15 LOH (cfr. microsatellites analysis) (n°15, 17, 18), whereas it was detected in the five other cases in either a few cells (four cases) or numerous cells (n°16) (Figs. 4*F*). It was always present in islets located outside both types of lesions (Figs. 4*G* and *H*).

**Microsatellites analysis.** A genetic map of microsatellites tested is given in Fig. 5. For informative cases, allelic loss is documented if one allele is significantly decreased (<50%) in cells from the lesions compared with the same allele coming from cells located outside the lesions. All tested cases of FoPHHI showed extensive 11p15 LOH involving imprinted genes in 11p15.5 and ABCC8 and KCNJ11 in 11p15.1. Interestingly, three of the eight insulinomas (n°15, 17, 18) showed LOH of a similar extent. However, importantly, these three insulinomas were not different from the five others for any other parameter studied (Fig. 2). DNA extraction efficacy is probably lower in formalin-fixed material rather than in frozen material, explaining the differences in microsatellites detection between cases.

## DISCUSSION

Severe hypoglycemic hyperinsulinemia characterizes FoPHHI and insulinoma and both are curable by selective surgical resection. The present study demonstrates that FoPHHI is a specific homogeneous entity contrasting with insulinoma but also that some insulinomas have a similar molecular background to FoPHHI.

The constant morphological aspect of the FoPHHI lesion is characterized by large endocrine clusters intermingled with exocrine tissue, whereas insulinomas of this series have the previously reported trabecular or solid pattern (29). Their cellular composition also differs: insulinomas are here almost exclusively composed of β-cells, whereas in FoPHHI, as in normal islets, non–β-cells always delineate β-cells cores. This difference is apparently not age-related. Indeed, our quantification demonstrates

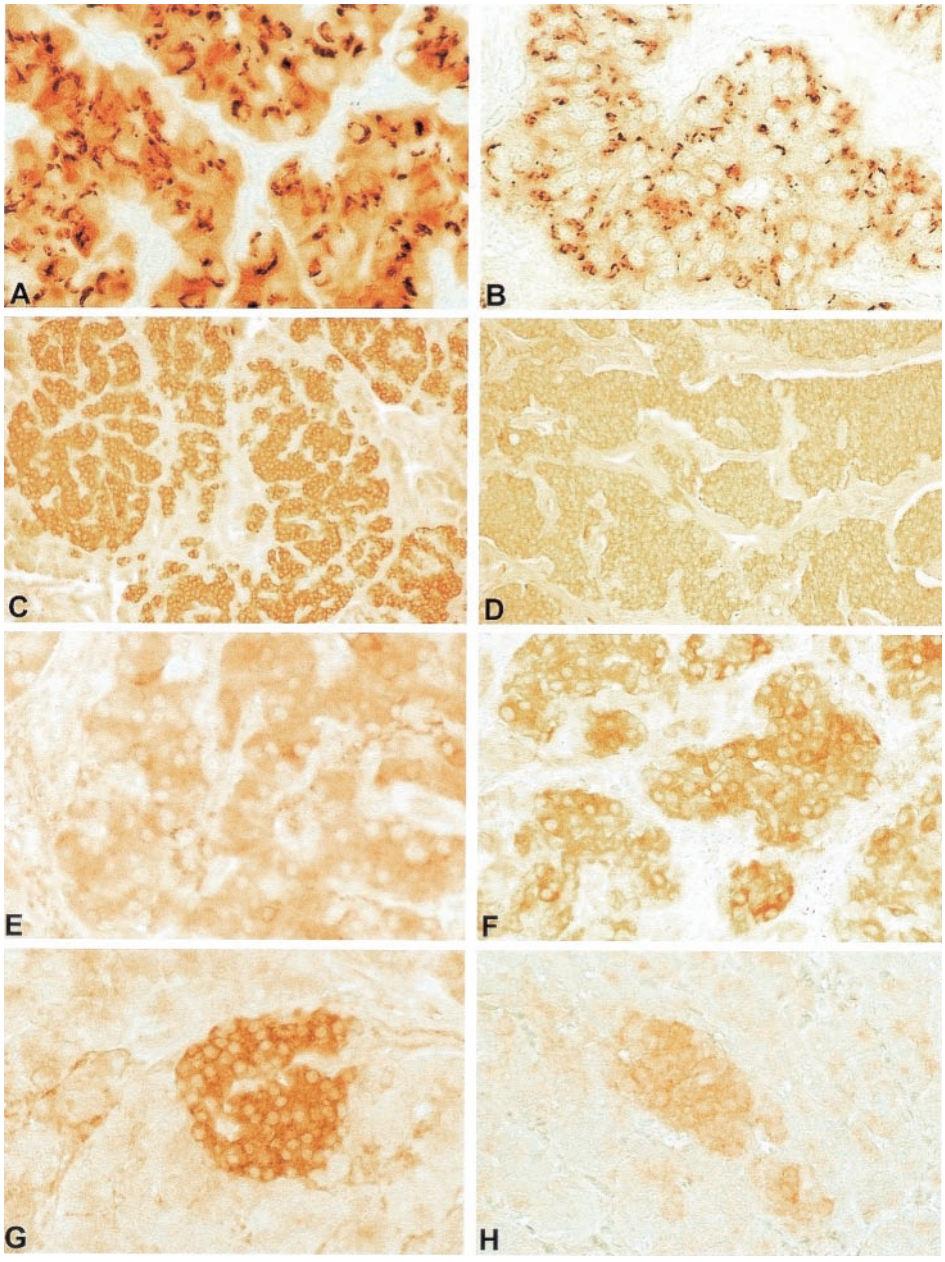


**FIG. 3. Morphological description of functional characteristics (*A*, *C*, *E*, and *G*: FoPHHI and *B*, *D*, *F*, and *H*: insulinoma). In all cases of FoPHHI, proinsulin labeling is very strong in an enlarged Golgi area but also to a lesser degree in the β-cells cytoplasm (*A*: case n°1, immunoperoxidase ×550). In insulinomas, this staining is less intense and restricted to a small Golgi area (*B*: case n°15, immunoperoxidase ×550). Proinsulin mRNA is detected in both lesions, but the staining was higher in FoPHHI (*C*: case n°11, peroxidase in situ hybridization ×125) than in insulinomas (*D*: case n°16, peroxidase in situ hybridization ×125). The staining for ABCC8 peptide is homogeneous and dense in the whole cytoplasm of endocrine cells in FoPHHI lesion (*E*: case n°3, immunoperoxidase ×250). However, this staining is clearly lower than that observed in islets outside the lesion (*G*: case n°3, immunoperoxidase ×250). On the contrary, this staining is stronger in insulinoma (*F*: case n°14, immunoperoxidase ×250) than in adjacent islets (*H*: case n°14, immunoperoxidase ×250).**

that β- and δ-cells proportions within both lesions differ from those outside lesions. Interestingly, islets outside insulinomas have a cellular composition identical to that of normoglycemic controls, whereas islets outside FoPHHI tend to have more δ-cells than normoglycemic controls. This may result from hyperinsulinemic hypoglycemia or reflect an immature development of these islets, which resemble those of neonates (27).

We also used various morphological approaches to evaluate several functional characteristics of both types of lesions. In this evaluation, FoPHHI appears very homogeneous. Indeed, compared with adjacent islets, all lesions have a high Golgi proinsulin/β-cell area, indicative of stimulated proinsulin production. In agreement with previous studies (30), there is no obvious abnormal prohormone processing. Interestingly, despite this high proinsulin production, proinsulin mRNA expression is not significantly different inside and outside the lesion. This is not due to limitations of our technique as its accuracy, reproducibility, and sensitivity previously have been demonstrated (25). This apparent discrepancy clearly indicates that in FoPHHI, proinsulin production regulation occurs at a translational rather than a transcriptional level in lesional β-cells. No significant differences in insulin storage were observed, although it appeared slightly lower within lesions. As lesional proinsulin production is over twice that outside, similar insulin content values imply its abnormal release. This is indeed what happens to β-cells without functional $K_{ATP}$ channels.

In insulinomas, insulin content, although variable, is consistently lower within the lesion than in surrounding islets. As previously reported (31), this could either result from low insulin production or from its abnormal release. Golgi proinsulin/β-cell area, although slightly larger inside the lesion, was not significantly different outside, and great individual variations were observed, in agreement with previous studies (32). Furthermore, diffuse cytoplasmic proinsulin labeling indicative of impaired proinsulin-insu-

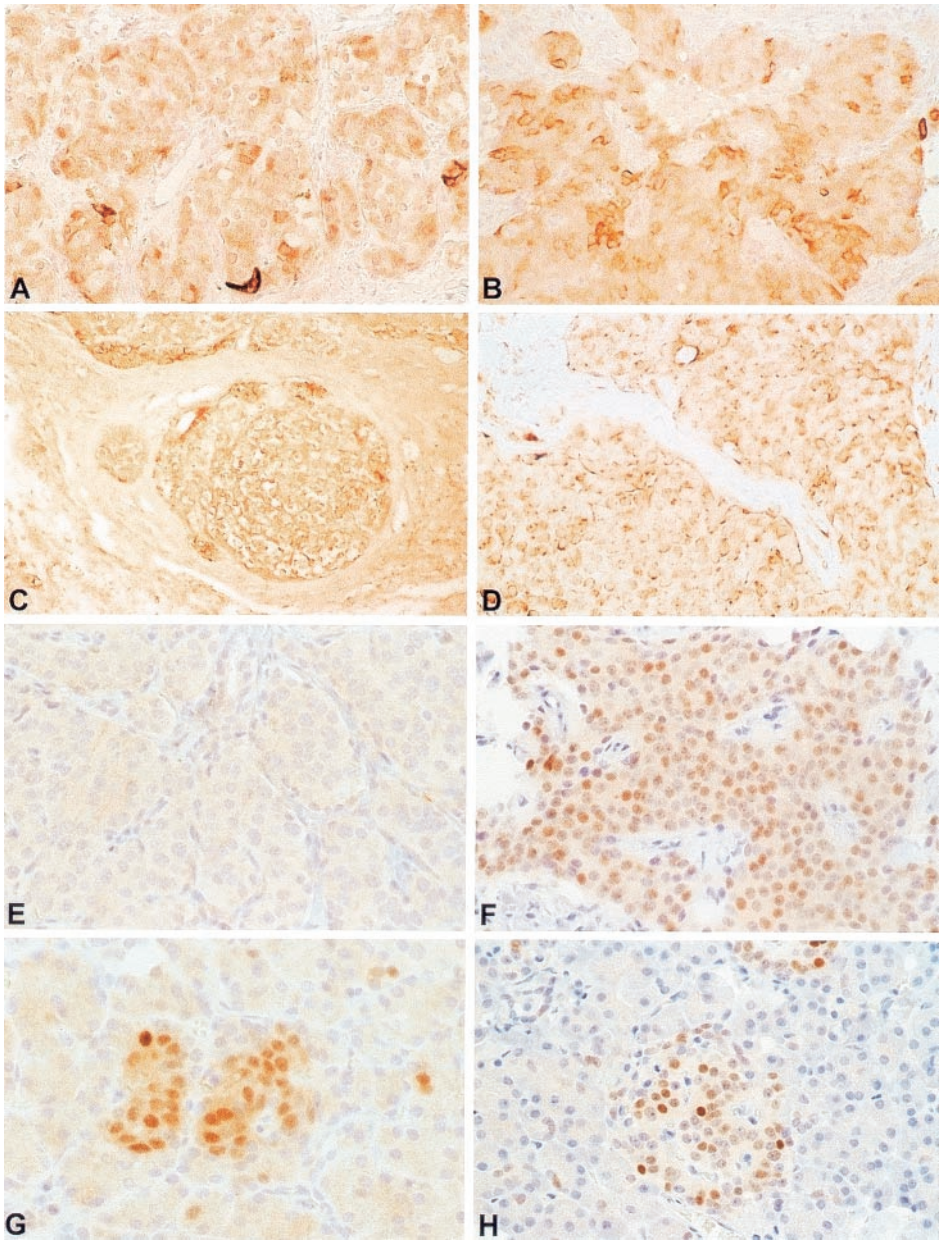


**FIG. 4. IGF2 and CDKN1C peptide expression in both types of lesions (*A*, *C*, *E*, and *G*: FoPHHI and *B*, *D*, *F*, and *H*: insulinoma). IGF2 peptide is immunodetected in FoPHHI lesion (*A*: case n°8, immunoperoxidase ×160) and also in insulinomas (*B*: case n°17, immunoperoxidase ×160). The staining is quite variable from cell to cell in both lesions. IGF2 mRNA is also detected in a majority of cells of FoPHHI lesion (*C*: case n°8, peroxidase in situ hybridization ×125) and insulinomas (*D*: case n°17, peroxidase in situ hybridization ×125). IGF2 peptide was also detected in islets outside both lesions whereas IGF2 mRNA was not (data not shown). CDKN1C peptide is completely absent from all tested cases of FoPHHI lesion (*E*: case n°7, immunoperoxidase ×350) and from insulinomas with 11p15 LOH (not shown). All insulinomas without LOH exhibit CDKN1C peptide nuclear staining either in a few number of cells or in numerous cells (*F*: case n°16, immunoperoxidase ×300). This peptide is present in islets located outside FoPHHI lesion (*G*: case n°7, immunoperoxidase ×350) and outside insulinomas (*H*: case n°16, immunoperoxidase ×300).**

lin conversion, was found in various tumoral cells of three cases, as previously reported in insulinomas (33). Proinsulin mRNA content was similar in insulinomas and adjacent islets, as in FoPHHI. However, proinsulin mRNA concentration was lower than in FoPHHI, suggesting a lower functional state.

Crowding measurement is another way of evaluating the functional state of endocrine cells. This parameter proved to be of major interest to differentiate focal and diffuse PHHI (4), even on per-operative sections (11). In FoPHHI, islets adjacent to the lesions have a resting appearance leading to high crowding, thereby reflecting the influence of permanent hyperinsulinemic hypoglycemia. Surprisingly, despite hyperinsulinemic hypoglycemias, islets located outside insulinomas have no resting appearance and no increased crowding. Several explanations are proposed. First, islets adjacent to FoPHHI endured hypoglycemia from birth, whereas those adjacent to insulinomas functioned normally for years. Second, counter-regulation mechanisms are more effective in adults than in infants and could reduce both severity and duration of hypoglycemias. Finally, our data indicate a very high proinsulin production in FoPHHI unobserved in insulinoma, which may thus result in more permanent, higher, and inadequate insulin release. Preoperative diazoxide treatment was only used in four of eight insulinomas and is thus unlikely involved in the differences observed between the islets.

This study is the first to report ABCC8 peptide expression in PHHI. The different expression in both lesions is interesting and surprising. Indeed, ABCC8 peptide amounts are significantly lower in FoPHHI and significantly higher in insulinomas than in their respective adjacent islets. Even the infants that could not be tested for *ABCC8* mutation were resistant to diazoxide treatment, a hallmark of $K_{ATP}$ channel dysfunction in hypersecreting β-cells. Assuming an *ABCC8* mutation was indeed present in all FoPHHI, the decrease in ABCC8 protein is in full agreement with lesional LOH. The indi-

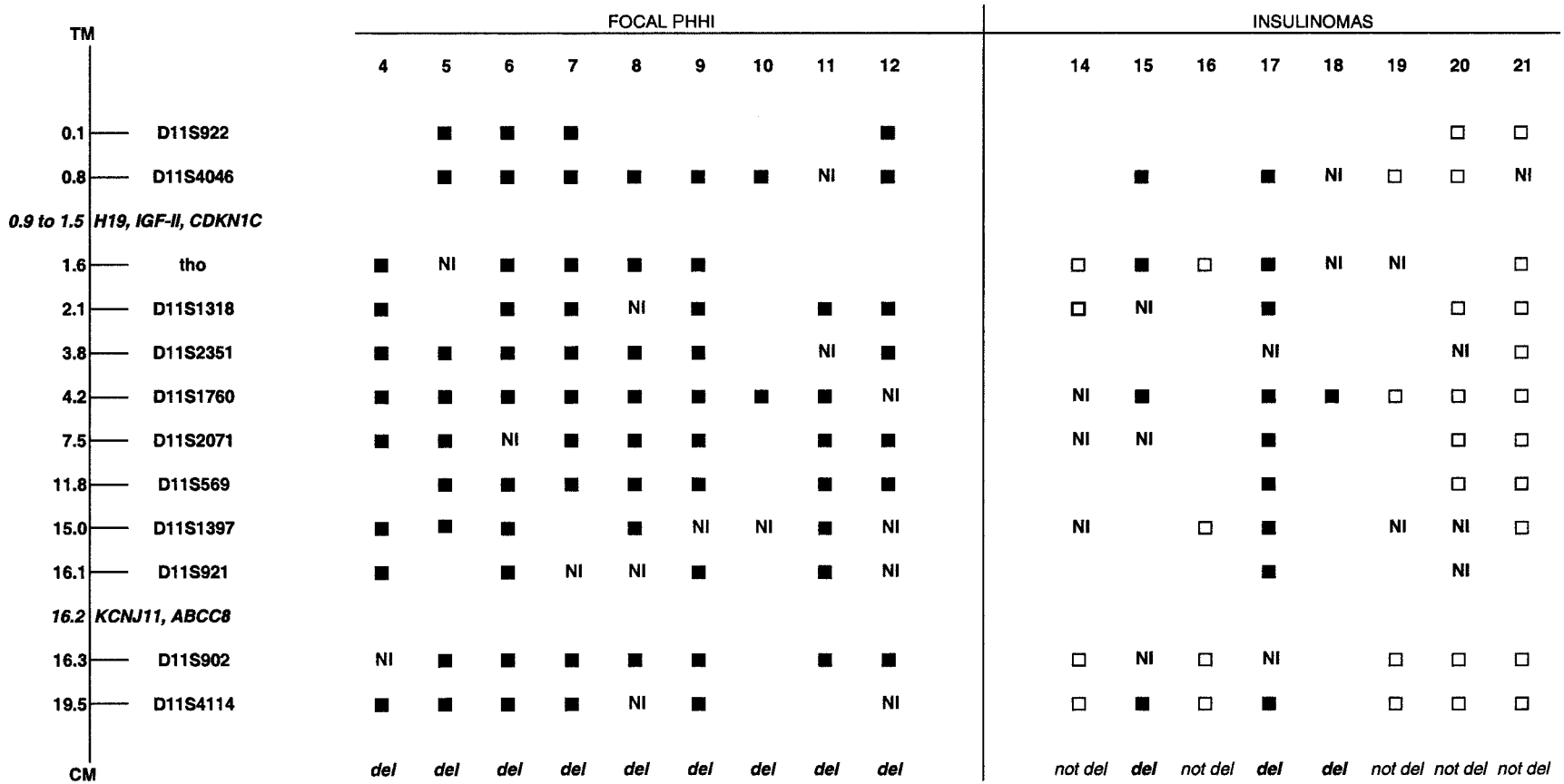


FIG. 5. Genetic map and microsatellites analysis. Microsatellites are indicated by their name. Their location on 11p15 is indicated by their distance from the centromere given in Mb. Genes are indicated in italics. The results are given for FoPHHI (cases n°4–12) and for insulinomas (cases n°14–21). ■, LOH; □, no LOH; NI, region was homozygous and did not allow the search for LOH. Within the lesion, all cases of FoPHHI show an extensive and homogeneous LOH of 11p15 region always involving imprinted genes in 11p15.5 and *ABCC8* and *KCNJ11* genes in 11p15.1. Three of the eight insulinomas show a LOH of similar extent (cases n°15, 17, and 18).

vidual differences probably reflect different mutations. Indeed, not all mutations lead to a truncated protein, and it is likely that in some cases (case n°2), the protein is still present but abnormal and nonfunctional.

The increased ABCC8 protein expression in insulinomas was unexpected. It could be a characteristic of those tumoral cells. However, it could also reflect the normal expression level and imply that immunolabeling of adjacent islets is actually below normal. As ABCC8 protein is present in similar amounts in islets outside both insulinomas and FoPHHI, this low expression could reflect an adaptative response to hypoglycemia. Functional consequences of the higher ABCC8 protein expression in insulinomas are unclear, as it does not prevent abnormal insulin release. Rather than an increased β-cell mass, an abnormal regulation of insulin secretion certainly explains hyperinsulinism in insulinomas, but the reasons for this are unclear. To our knowledge, the eventual implication of *ABCC8* mutations in insulinomas has never been studied. The increased ABCC8 peptide labeling findings in insulinomas in our series does not necessarily imply that the peptide functions normally. However, the fact that four of eight insulinomas of this series were sensitive to diazoxide does not favor the *ABCC8* hypothesis.

The characteristic organization of the FoPHHI lesion with its islet-like pattern is indicative of adenomatous hyperplasia. The previously reported increased β-cell proliferation (18,19) could result from localized growth stimulating factors or from loss of local inhibitory mechanisms (1). This is in total agreement with 11p15 LOH observed in all of our FoPHHI and in those previously published (12–14). Indeed, this LOH changes the expression of 11p15 imprinted genes, resulting in an imbalance of corresponding gene products that could lead to excessive β-cell proliferation and adenomatous hyperplasia. In this region, maternally expressed *H19* and *CDKN1C* genes and paternally expressed *IGF2* (34–36) are known to play an important role in cell proliferation. *IGF2* has been implicated in β-cell hyperplasia as shown in transgenic mice overexpressing this gene (37,38). Our investigations demonstrated similar amounts of *IGF2* peptide in FoPHHI and adjacent islets, whereas IGF2 mRNA was only present within the lesion. This discrepancy between IGF2 peptide and mRNA has previously been reported for Wilms' tumors and pheochromocytomas (24,39). This could result from accelerated degradation or from nonregulated excessive secretion of the peptide. In contrast to our results, Kassem et al. (40) report increased IGF2 peptide amounts in FoPHHI. However, this increase is weak, and discrepancies between the two studies could be explained by the differences in measurement methods. Indeed, we mainly observed IGF2 in β-cells but sometimes also in non–β-cells, as reported for fetal pancreases (41). We then chose an antibody against synaptophysin, a general endocrine marker (42), and not insulin for measuring the reference area in order to avoid restricting reference area to β-cells alone, contrary to Kassem et al. (40). Furthermore, synaptophysin identifies endocrine cells, whatever their functional state, because its detection is independent of the presence of granules. Our detection of IGF2 mRNA restricted to the lesion seems to contradict Fournet et al. (13), who could not demonstrate by semiquantitative RT-PCR assay an increased IGF2 mRNA concentration within the lesion. This difference may again be explained by different mRNA detection methods. Indeed, small differences in mRNA content could escape large RT-PCR amplification but be detected by less sensitive but accurate in situ hybridization. Furthermore, this last technique offers the opportunity to analyze which cell type contains mRNA. Presence of IGF2 in insulinomas has previously been reported (43). Interestingly, the pattern of IGF2 peptide and mRNA expression is similar in insulinomas and FoPHHI. We can thus conclude from our results that IGF2 overexpression exists at mRNA level in both lesions.

The function of *H19* gene is still unclear, one proposition being that it directly or indirectly modulates IGF2 mRNA cytoplasmic levels (44). As both FoPHHI and insulinomas (with or without LOH) equally expressed IGF2, *H19* is likely to play a role by itself, its loss combined with *IGF2* overexpression, explaining previously reported differences in β-cell proliferation (18). In agreement with this interpretation, Fournet et al. (13) found a decreased expression of the *H19* gene in FoPHHI and proposed that *IGF2/H19* imbalance rather than *IGF2* upregulation induced pancreatic hyperplasia in FoPHHI.

Interestingly, three of our eight insulinomas had the same 11p15 LOH as all FoPHHI cases. This LOH is thus not so exceptional in insulinomas. It was indeed already reported on the basis of a long deletion involving the whole length of chromosome 11 (21). In our study, the long arm of chromosome 11 was not analyzed. A more recent paper (22), using another technique based on DNA copies quantification, also demonstrated 11p15 LOH in some insulinomas. Although molecular background and tumoral mechanisms certainly appear more heterogeneous in insulinomas, they may be similar to FoPHHI in cases with 11p15 LOH.

Finally, molecular homogeneity in FoPHHI is further supported by the constant loss of CDKN1C peptide expression in our series, as recently published by Kassem et al. (40). This gene encodes for a cyclin-dependent kinase inhibitor and is a negative cell proliferation regulator (45) implicated in the pathogenesis of several tumors (17). 11p15 LOH results in loss of the protein, this loss potentially also playing a role in the occurrence of the lesion. CDKN1C peptide is also absent in insulinomas with 11p15 LOH, whereas it is always present in insulinomas devoid of LOH, indicating, as proposed by Kassem et al. (40), its potential usefulness in tumoral 11p15 LOH detection.

In conclusion, this study, combining morphology with quantitative and molecular data demonstrates the extraordinarily homogeneous character of FoPHHI. This hyperplastic lesion, likely resulting from an imbalance between 11p15 imprinted gene products related to constant LOH of this region, produces great amounts of proinsulin in response to abnormal insulin release consecutive to decreased ABCC8 peptide expression. Adjacent islets are resting, and their composition is similar to that of normoglycemic neonates. These results evidence intra-pancreatic regulation of islet β-cell activity at a translational level. In accordance with previous studies, we confirm the heterogeneity of insulinomas. Therefore, FoPHHI is not an insulinoma of the infant, although some insulinomas share molecular background similarities.

**ACKNOWLEDGMENTS**

This study was supported by FRSM Belgium (Grant no. 3.4594.99) and by the European Network for Research into Hyperinsulinism in Infancy (ENRHI).

The authors thank Dr. Michael Mikhailov and Prof. Steve Ashcroft for the gift of the antibody against *ABCC8* peptide. They also thank Mr. Stéphane Lagasse for his precious help in preparing the photomicrographs and Dr. Claire de Burbure for reviewing the manuscript.

**REFERENCES**

1. Jaffe R, Hashida Y, Yunis EJ: Pancreatic pathology in hyperinsulinemic hypoglycemia of infancy. *Lab Invest* 42:356–365, 1980
2. Rahier J, Fält K, Müntefering H, Becker K, Gepts W, Falkmer S: The basic structural lesion of persistent neonatal hypoglycemia with hyperinsulinism: deficiency of pancreatic D cells or hyperactivity of B cells? *Diabetologia* 26:282–289, 1984
3. Goossens A, Gepts W, Saudubray JM, Bonnefont JP, Nihoul-Fékété C, Heitz PU, Klöppel G: Diffuse and focal nesidioblastosis: a clinicopathological study of 24 patients with persistent neonatal hyperinsulinemic hypoglycemia. *Am J Surg Pathol* 13:766–775, 1989
4. Sempoux C, Guiot Y, Lefèvre A, Nihoul-Fékété C, Jaubert F, Saudubray JM, Rahier J: Neonatal hyperinsulinemic hypoglycemia: heterogeneity of the syndrome and keys for differential diagnosis. *J Clin Endocrinol Metab* 83:1455–1461, 1998
5. de Lonlay-Debeney P, Poggi-Travert F, Fournet JC, Sempoux C, Vici CD, Brunelle F, Touati G, Rahier J, Junien C, Nihoul-Fékété C, Robert JJ, Saudubray JM: Clinical features of 52 neonates with hyperinsulinism. *N Engl J Med* 340:1169–1175, 1999
6. Thomas PM, Cote GJ, Wohllk N, Haddad B, Mathew PM, Rabl W, Aguilar-Bryan L, Gagel RF, Bryan J: Mutations in the sulfonylurea receptor gene in familial persistent hyperinsulinemic hypoglycemia of infancy. *Science* 268:426–429, 1995
7. Thomas P, Ye Y, Lightner E: Mutation of the pancreatic islet inward rectifier Kir 6.2 also leads to familial persistent hyperinsulinemic hypoglycemia of infancy. *Hum Mol Genet* 5:1809–1812, 1996
8. Aguilar-Bryan L, Nichols C, Wechsler S, Clement J, Boyd A, Gonzalez G, Herrera Sosa H, Nguy K, Bryan J, Nelson D: Cloning of the beta cell high-affinity sulfonylurea receptor: a regulator of insulin secretion. *Science* 268:423–426, 1995
9. Kane C, Shepherd RM, Squires PE, Johnson PR, James RF, Milla PJ, Aynsley-Green A, Lindley KJ, Dunne MJ: Loss of functional K+ATP channels in pancreatic B-cells causes persistent hyperinsulinemic hypoglycemia of infancy. *Nat Med* 2:1344–1347, 1996
10. Dunne MJ, Kane C, Shepherd RM, Sanchez JA, James RF, Johnson P, Aynsley-Green A, Lu S, Clement J, Lindley K, Seino S, Aguilar-Bryan L: Familial persistent hyperinsulinemic hypoglycemia of infancy and mutations in the sulfonylurea receptor. *N Engl J Med* 336:703–706, 1997
11. Rahier J, Sempoux C, Fournet JC, Poggi F, Brunelle F, Nihoul-Fékété C, Saudubray JM, Jaubert F: Partial or near-total pancreatectomy for persistent neonatal hyperinsulinemic hypoglycemia: the pathologist's role. *Histopathology* 32:15–19, 1998
12. Verkarre V, Fournet JC, de Lonlay P, Gross-Morand MS, Devillers M, Rahier J, Brunelle F, Robert JJ, Nihoul-Fékété C, Saudubray JM, Junien C: Paternal mutation of the sulfonylurea receptor (*SUR1*) gene and maternal loss of 11p15 imprinted genes lead to persistent hyperinsulinism in focal adenomatous hyperplasia. *J Clin Invest* 102:1286–1291, 1998
13. Fournet JC, Mayaud C, de Lonlay P, Gross-Morand MS, Verkarre V, Castanet M, Devillers M, Rahier J, Brunelle F, Robert JJ, Nihoul-Fékété C, Saudubray JM, Junien C: Unbalanced expression of 11p15 imprinted genes in focal form of congenital hyperinsulinism: association with a reduction to homozygosity of a mutation in *ABCC8* or *KCNJ11*. *Am J Pathol* 158:2177–2184, 2001
14. de Lonlay P, Fournet JC, Rahier J, Gross-Morand MS, Poggi-Travert F, Foussier V, Bonnefont JP, Brusset MC, Brunelle F, Robert JJ, Nihoul-Fékété C, Saudubray JM, Junien C: Somatic deletion of the imprinted 11p15 region in sporadic persistent hyperinsulinemic hypoglycemia of infancy is specific of focal adenomatous hyperplasia and endorses partial pancreatectomy. *J Clin Invest* 100:802–807, 1997
15. Ohlsson R, Nystrom A, Pfeifer-Ohlsson S, Tohonen V, Hedborg F, Schofield P, Flam F, Ekstrom T: *IGF2* is parentally imprinted during human embryogenesis and in the Beckwith-Wiedemann syndrome. *Nat Genet* 4:94–97, 1993
16. Moulton T, Crenshaw T, Hao Y, Moosikasuwan J, Lin N, Dembitzer F, Hensle T, Weiss L, McMorrow L, Loew T, Draus W, Gerals W, Tycko B: Epigenetic lesions at the *H19* locus in Wilms' tumour patients. *Nat Genet* 7:440–447, 1994
17. Hatada I, Inazawa J, Abe T, Nakayama M, Kaneko Y, Jinno Y, Niikawa N, Ohashi H, Fukushima Y, Iida K, Yutani C, Takahashi S, Chiba Y, Ohishi S, Mukai T: Genomic imprinting of human $p57^{KIP2}$ and its reduced expression in Wilms' tumors. *Hum Molec Genet* 5:783–788, 1996
18. Sempoux C, Guiot Y, Dubois D, Nollevaux MC, Sudubray JM, Nihoul-Fékété C, Rahier J: Pancreatic B-cell proliferation in persistent hyperinsulinemic hypoglycemia of infancy: an immunohistochemical study of 18 cases. *Modern Pathol* 11:444–449, 1998
19. Kassem SA, Ariel I, Thornton PS, Scheimberg I, Glaser B: Beta-cell proliferation and apoptosis in the developing normal human pancreas and in hyperinsulinism of infancy. *Diabetes* 49:1325–1333, 2000
20. Glaser B, Thornton P, Otonkoski T, Junien C: Genetics of neonatal hyperinsulinism. *Arch Dis Child Fetal Neonatal Ed* 82:F79–F86, 2000
21. Patel P, O'Rahilly S, Buckle V, Nakamura Y, Turner RC, Wainscoat JS: Chromosome 11 allele loss in sporadic insulinoma. *J Clin Pathol* 43:377–378, 1990
22. Stumpf E, Aalto Y, Höög A, Kjellman M, Otonkoski T, Knuutila S, Andersson LC: Chromosomal alterations in human pancreatic endocrine tumors. *Genes Chromosomes Cancer* 29:83–87, 2000
23. Service FJ, McMahon MM, O'Brien PC, Ballard DJ: Functioning insulinoma-incidence, recurrence, and long-term survival of patients: a 60-year study. *Mayo Clin Proc* 66:711–719, 1991
24. Haselbacher GK, Irminger JC, Zapf J, Ziegler WH, Humbel RE: Insulin-like growth factor II in human adrenal pheochromocytomas and Wilms tumors: expression at the mRNA and protein level. *Proc Natl Acad Sci* 84:1104–1106, 1987
25. Guiot Y, Rahier J: Validation of non radioactive in situ hybridization as a quantitative approach of messenger ribonucleic acid variations: a comparison with Northern Blot. *Diagn Mol Pathol* 6:261–266, 1997
26. vonWasielewski R, Mengel M, Gignac S, Wilkens L, Werner M, Georgii A: Tyramine amplification technique in routine immunohistochemistry. *J Histochem Cytochem* 45:1455–1459, 1997
27. Rahier J, Wallon J, Henquin JC: Cell populations in the endocrine pancreas of human neonates and infants. *Diabetologia* 20:540–546, 1981
28. Rahier J, Stevens M, De Menten Y, Henquin JC: Methods in laboratory investigations: determination of antigen concentration in tissue sections by immunodensitometry. *Lab Invest* 61:357–363, 1989
29. Berger M, Bordi C, Cüppers HJ, Berchtold P, Gries FA, Münterfering H, Sailer R, Zimmermann H, Orci L: Functional and morphologic characterization of human insulinomas. *Diabetes* 32:921–931, 1983
30. Leibowitz G, Weintrob N, Pikarsky A, Josefsberg Z, Landau H, Glaser B, Hales CN, Cerasi E: Normal proinsulin processing despite beta-cell dysfunction in persistent hyperinsulinemic hypoglycemia of infancy (nesidioblastosis). *Diabetologia* 39:1338–1344, 1996
31. Bani Sacchi T, Bani D, Biliotti G: The endocrine pancreas in patients with insulinomas: an immunocytochemical and ultrastructural study of the nontumoral tissue with morphometrical evaluations. *Int J Pancreatol* 5:11–28, 1989
32. Roth J, Klöppel G, Madsen OD, Storch MJ, Heitz PU: Distribution patterns of proinsulin and insulin in human insulinomas: an immunohistochemical analysis in 76 tumors. *Virchows Archiv B Cell Pathol* 63:51–61, 1992
33. Roth J, Komminoth P, Heitz PU: Topographic abnormalities of proinsulin to insulin conversion in functioning human insulinomas: comparison of immunoelectron microscopic and clinical data. *Am J Pathol* 147:489–502, 1995
34. Rachmilewitz J, Goshen R, Ariel Ilana, Schneider T, de Groot N, Hochberg A: Parental imprinting of the human *H19* gene. *FEBS* 309:25–28, 1992
35. Giannoukakis N, Deal C, Paquette J, Goodyer CG, Polychronakos C: Parental genomic imprinting of the human *IGF2* gene. *Nat Genet* 4:98–101, 1993
36. Matsuoka S, Thompson JS, Edwards MC, Barletta JM, Grundy P, Kalikin LM, Harper JW, Elledge SJ, Feinberg AP: Imprinting of the gene encoding a human cyclin-dependent-kinase inhibitor, p57(KIP2), on chromosome 11p15. *Proc Nat Acad Sci* 93:3026–3030, 1996
37. Petrik J, Pell JM, Arany E, McDonald TJ, Dean WL, Reik W, Hill DJ: Overexpression of insulin-like growth factor II in transgenic mice is associated with pancreatic islet cell hyperplasia. *Endocrinology* 140:2353–2363, 1999
38. Devedjian JC, George M, Casellas A, Pujol A, Visa J, Pelegrin M, Gros L, Bosch F: Transgenic mice overexpressing insulin-like growth factor II in β cells develop type 2 diabetes. *J Clin Invest* 105:731–740, 2000

39. Baccarini P, Fiorentino M, D'Errico A, Mancini AM, Grigioni WF: Detection of anti-sense transcripts of the insulin-like growth factor-2 gene in Wilms' tumor. *Am J Pathol* 143:1535–1542, 1993
40. Kassem SA, Ariel I, Thornton PS, Hussain K, Smith V, Lindley KJ, Aynsley-Green A, Glaser B: p57KIP2 expression in normal islet cells and in hyperinsulinism of infancy. *Diabetes* 50:2763–2769, 2001
41. Portela-Gomes GM, Höög A: Insulin-like growth factor II in human fetal pancreas and its co-localization with the major islet hormones: comparison with adult pancreas. *J Endocrinol* 165:245–251, 2000
42. Capella C, Heitz PU, Höfler H, Solcia E, Klöppel G: Revised classification of neuroendocrine tumors of the lung, pancreas and gut. *Virchows Archiv* 425:547–560, 1995
43. Höög A, Kjellman M, Sandberg Nordqvist AC, Höög CM, Juhlin C, Falkmer S, Schalling M, Grimelius L: Insulin-like growth factor-II in endocrine pancreatic tumours. *APMIS* 109:127–140, 2001
44. Li YM, Franklin G, Cui HM, Svensson K, He XB, Adan G, Ohlsson R, Pfeifer S: The *H19* transcript is associated with polysomes and may regulate *IGF2* expression in trans. *J Biol Chem* 273:28247–28252, 1998
45. Matsuoka S, Edwards M, Bai C, Parker S, Zhang P, Baldini A, Harper J, Elledge S: p57KIP2, a structurally distinct member of the p21CIP1 Cdk inhibitor family is a candidate tumor suppressor gene. *Genes Dev* 9:650–662, 1995